Projectile angular-differential cross sections for transfer and transfer excitation in proton collisions with helium

M. Zapukhlyak* and T. Kirchner†
Institut für Theoretische Physik, TU Clausthal, D-38678 Clausthal-Zellerfeld, Germany

A. Hasan
Physics Department and Laboratory for Atomic, Molecular, and Optical Research, Missouri University of Science and Technology, Rolla, Missouri 65401, USA
and Department of Physics, UAE University, P.O. Box 17551, Alain, Abu Dhabi, United Arab Emirates

B. Tooke and M. Schulz
Physics Department and Laboratory for Atomic, Molecular, and Optical Research, Missouri University of Science and Technology, Rolla, Missouri 65401, USA

(Received 26 September 2007; published 28 January 2008)

Projectile angular-differential cross sections for single-transfer and transfer excitation have been calculated with the two-center extension of the nonperturbative basis generator method for 5–200 keV proton-helium collisions. The calculations are based on the independent electron model, and the eikonal approximation has been used to extract angular-differential cross sections from impact-parameter-dependent transition amplitudes. The present results are compared with experimental and previous theoretical data where available. In particular, we consider the ratio of transfer excitation to single capture versus double excitation to single excitation at intermediate energies. An experimentally observed structure in this ratio at a scattering angle about 0.5 mrad is qualitatively reproduced, while a previous classical evaluation failed in this respect. Therefore, we conclude that this structure is caused by quantum mechanical heavy-particle-electron couplings.

DOI: 10.1103/PhysRevA.77.012720 PACS number(s): 34.50.Fa, 34.50.−s, 34.70.+e

I. INTRODUCTION

Studies of the fundamental interactions between ions and atoms constitute a significant and important part of contemporary atomic physics. In this work we are trying to elucidate some features of the few-particle dynamics in p-He collisions. Usage of helium as target species remains probably the best compromise between simplicity desired from a numerical point of view and the complexity that is unavoidable in studying the dynamics of many-electron processes. In spite of much evidence for the importance of electron-electron (e-e) correlation effects in this system, the capabilities and limitations of uncorrelated theories have remained somewhat unclear, since even on this level accurate numerical solutions are difficult and sparse. Incorporation of e-e correlations for dynamical ion-atom scattering is, of course, an even more complicated problem such that the question, when and where specific processes can be viewed as uncorrelated, has not received a satisfying answer, yet. It is well known that even the seemingly simple single-transfer (ST) process consists not only of a plain interaction of the projectile and one of the target electrons, but is in general a more complicated process. For instance, multiple scattering mechanisms known as the (classical) Thomas processes of the first and second kind can be important at high collision energies in the MeV regime [1]. The former involves the scattering of the projectile from the electron and subsequent scattering of this electron from the target (P-e-T), while the latter consists of the scattering of the projectile from the first electron and subsequent scattering of the first electron from the second one (P-e-e). Both processes can result in capture of one electron and give a characteristic peak structure in the angular-differential cross sections (DCS) at around $\theta=0.47$ and 0.55 mrad, respectively. If the state of the second electron is controlled (i.e., fixed to the ground state), the P-e-e process does not occur.

Theoretically the single-electron transfer DCS in p-He collisions has been investigated in many studies. Recent results and rather comprehensive lists of previous publications can be found, e.g., in the papers by Mančev *et al.* [2] and Abufager *et al.* [3]. We only note that the majority of those works are based on the Born distorted wave (BDW) and continuum distorted wave theories and their derivatives, which work well at relatively high impact energy E_P. Below $E_P \approx 100$ keV the total cross section (TCS) for ST is typically overestimated significantly. In the low and intermediate energy region the coupled-channel atomic orbital (AO) and molecular orbital (MO) methods are more adequate and give in general a better account of experimental data. At low energies ($E_P < 5$ keV) the molecular nature of the collision system becomes apparent. The calculation of ST DCS for $E_P=0.5-5$ keV has been successfully carried out with the MO approach in the work of Johnson *et al.* [4]. At intermediate energies the collision time becomes too short to allow the electrons to form well-defined molecular states, and the AO expansion methods are superior. Such calculations have been performed, e.g., by Slim *et al.* [5] and Martin *et al.* [6].

Processes involving multiple electronic transitions tend to be much more difficult to be studied, both experimentally

*myroslaw.zapukhlyak@tu-clausthal.de
†tom.kirchner@tu-clausthal.de

and theoretically. However, in the last decade the experimental possibilities have grown significantly due to development and elaboration of the COLTRIMS (cold target recoil ion momentum spectroscopy), sometimes also called reaction microscope, technique [7,8]. In this approach, the momentum distribution of the recoil ions is measured (depending on the specific experiment in coincidence with one or more ejected electrons or with the scattered projectile) and the momentum distribution of undetected particles can be deduced from momentum conservation.

Recently, intermediate energy p-He collisions (25–75 keV) were studied with COLTRIMS, and for the first time angular-differential cross sections for transfer excitation (TE) were reported [9]. In combination with ST, double excitation (DE) (measured earlier [10,11]) and single excitation (SE) data the ratio R of TE/ST to DE/SE

$$R = \frac{\mathrm{TE}}{\mathrm{ST}} \Big/ \frac{\mathrm{DE}}{\mathrm{SE}} \tag{1}$$

was compared with calculations based on the semiclassical approximation using the ansatz of Greenland [12], in which the DCS for any inelastic process is a product of the DCS for classical elastic scattering and the electronic transition probability for the analyzed process x,

$$\frac{d\sigma_{\mathrm{in}}}{d\Omega(\theta)} = \frac{d\sigma_{\mathrm{el}}}{d\Omega(\theta)} P_x(\theta). \tag{2}$$

The two-electron transition probabilities were calculated within the independent electron model (IEM), i.e., by combining single-electron transition probabilities according to multinomial statistics. This has been done to investigate to what extent the data can be explained without incorporating any e-e correlation effect. The single-electron calculations were performed by using the two-center (TC) extension of the basis generator method (BGM) introduced recently [13]. The calculated DCS themselves were not unreasonable, but significant discrepancies to the measurements became apparent for the ratio (1). If one uses the same classical scattering potential for all processes x one obtains $R \equiv 2$ within the IEM [9]. In contrast, the experimental ratio R at $E_P = 50$ keV exhibits a structure around a scattering angle of $\theta = 0.5$ mrad. When using different scattering potentials for the different processes the calculated ratio is also no longer constant, but shows a monotonic increase as a function of θ and reaches 2 only asymptotically [9]. The experimentally observed peak structure is completely absent. It was therefore concluded that it must be caused by dynamic nucleus-electron couplings beyond the simple model used and/or e-e correlation effects. Since both possible sources of error could not be disentangled the limits of the IEM could not be assessed with certainty.

It is one of the goals of the present paper to clarify this question and to explain the peak structure in R at least on a qualitative level. We keep the IEM, which means that in our present calculation e-e correlations are not included. But instead of using the classical ansatz (2) we translate the impact-parameter-dependent transition amplitudes obtained from TC-BGM calculations to angular-differential cross sections by applying the well-known eikonal method [14–16]. In this way quantum effects are taken into account in the heavy-particle scattering, and this turns out to be important. To validate our approach we have calculated DCS for ST over a wider range of impact energies and present our results in comparison with experimental data. Two models are applied to construct the impact-parameter-dependent transition amplitudes for the one-electron processes ST and SE, which shed some further light on the validity and limitations of the IEM.

Atomic units ($\hbar = m_e = e = 1$) are used unless indicated otherwise.

II. THEORY

Our starting point for the theoretical description of the (nonrelativistic) collision problem is the semiclassical approximation: We assume that the electronic and nuclear motions can be separated, and the influence of the latter on the former can be described in terms of classically moving charges. The Hamiltonian of the system is written as

$$\hat{H} = \hat{H}_e + V_{nn}, \tag{3}$$

where $V_{nn} = \frac{Z_p Z_t}{R}$ is the Coulomb repulsion between the projectile and the target nucleus with charges Z_p and Z_t, respectively. Since we assume a straight-line trajectory with impact parameter b and constant velocity v the internuclear distance is given as $R = \sqrt{b^2 + (vt)^2}$. Within the IEM $\hat{H}_e$ is approximated as a sum of single-electron Hamiltonians

$$\hat{H}_e \approx \sum_{i=1}^{N} \hat{h}_i, \tag{4}$$

such that the many-electron wave function can be represented as an antisymmetrized product wave function with orbitals that solve time-dependent Schrödinger equations (TDSE)

$$i\partial_t \psi_i(\mathbf{r},t) = \hat{h}\psi_i(\mathbf{r},t), \quad i = 1, \ldots, N \tag{5}$$

driven by the single-particle Hamiltonian

$$\hat{h} = -\frac{1}{2}\Delta + V_{\mathrm{He}}(r_t) - \frac{Z_p}{r_p} \tag{6}$$

that contains the kinetic energy and (effective) target and projectile potentials. r_t and $r_p = |\mathbf{r}_t - \mathbf{R}|$ denote the distances between electron and target and projectile centers, respectively. For $V_{\mathrm{He}}(r_t)$ we use an accurate helium ground-state potential obtained from the optimized potential method [17]. It includes the Hartree and exact exchange potentials, but no correlation contribution. For solving the TDSE we use the BGM, a nonperturbative coupled-channel method that includes basis states which structurally adapt to the dynamics of the collision problem [18,19]. It was successfully applied to a broad range of dynamical collision problems over the years [20] and has recently been extended to a two-center formulation (TC-BGM) [13]. The TC-BGM basis consists of a finite set of U_t target and $U - U_t$ projectile states (in our

case all orbitals of the *KLMN* shells). Galilean invariance is taken into account by the appropriate choice of electron translation factors

$$\phi_u^0(\mathbf{r}) = \begin{cases} \phi_u(\mathbf{r}_t)\exp(i\mathbf{v}_t\mathbf{r}), & u \le U_t, \\ \phi_u(\mathbf{r}_p)\exp(i\mathbf{v}_p\mathbf{r}), & \text{otherwise.} \end{cases} \tag{7}$$

Here, $\mathbf{v}_t$ and $\mathbf{v}_p$ denote the constant velocities of the atomic target and projectile frames in the center-of-mass frame, respectively. Equation (7) defines a standard two-center AO expansion. It is augmented by BGM states, which are constructed by repeated application of a regularized projectile potential onto the target states [19]

$$\chi_u^\mu(\mathbf{r},t) = [W_p(t)]^\mu \phi_u^0(\mathbf{r}), \quad \mu = 1, \ldots, M, \quad u = 1, \ldots, U_t, \tag{8}$$

$$W_p(t) = \frac{1}{|\mathbf{r}_t - \mathbf{R}(t)|}\{1 - \exp[-|\mathbf{r}_t - \mathbf{R}(t)|]\}. \tag{9}$$

The set of pseudostates of Eq. (8) when orthogonalized to the generating two-center AO basis (7) accounts for ionization channels and for quasimolecular effects at low collision velocity, which cannot be described by standard two-center AO expansions. In the present work the basis includes 51 functions from the set $\{\chi_u^\mu(\mathbf{r},t), \mu \ge 1, u \le U_t\}$ up to order $\mu=5$ in addition to the bound target and projectile states.

Within the IEM for a closed-shell two-electron system, as with He two-electron transition amplitudes are given as products of single-electron transition amplitudes $a_{if} = \langle \phi_f | \psi_i \rangle|_{t\to\infty}$ and a factor that accounts for the indistinguishability of the electrons. Accordingly, we have calculated the two-electron amplitudes for TE and DE processes as

$$a_{IF}^{\mathrm{TE}} = \sqrt{2} a_{if}^T a_{if'}^E, \tag{10}$$

$$a_{IF}^{\mathrm{DE}} = \begin{cases} \sqrt{2} a_{if}^E a_{if'}^E, & f \ne f', \\ a_{if}^E a_{if'}^E, & f = f'. \end{cases} \tag{11}$$

A similar model was successfully applied to transfer-ionization processes in the *p*-He collision system by Gayet and Salin [21]. Note that the two-electron amplitudes (10) and (11) correspond to the usual transition probabilities in the IEM, e.g.,

$$P^{\mathrm{TE}} = |a_{IF}^{\mathrm{TE}}|^2 = 2|a_{if}^T|^2 |a_{if'}^E|^2 = 2P^T P^E. \tag{12}$$

In the experiments for ST and SE the final state of the second electron is typically fixed to the ground state. Correspondingly, we have calculated the ST and SE amplitudes as

$$a_{IF}^{\mathrm{ST}} = \sqrt{2} a_{if}^T a_{ii}^{1s} \tag{13}$$

$$a_{IF}^{\mathrm{SE}} = \sqrt{2} a_{if}^E a_{ii}^{1s}, \tag{14}$$

where a_{ii}^{1s} is the amplitude for finding the second electron in the target ground state.

In order to extract angular-dependent scattering amplitudes $f_{IF}(\theta)$ from the impact-parameter-dependent transition amplitudes $a_{IF}(b)$, we use the eikonal approximation. This method reintroduces quantum mechanics in the heavy-particle scattering despite the assumption of straight-line trajectories in the electronic Hamiltonian. It was described in detail by McCarroll and Salin [14], Wilets and Wallace [15], and Glauber [16], and has been applied to ion-atom collision problems in many studies with considerable success. A two-dimensional Fourier transformation is required to obtain the eikonal scattering amplitude $f_{IF}^E(\theta)$, and after carrying out the azimuthal integration the amplitude is given by [22]

$$f_{IF}^E(\theta) = ik_i \int_0^\infty b J_{\Delta M}\left(2k_i b \sin\frac{\theta}{2}\right) A_{IF}(b) db, \quad I \ne F, \tag{15}$$

where k_i is the initial momentum of the projectile, $\Delta M = |m_i - m_f|$ is the difference of the initial- and final-state magnetic quantum numbers, and $J_{\Delta M}$ is a Bessel function. $A_{IF}(b)$ is the impact-parameter-dependent electronic transition amplitude $a_{IF}(b)$ multiplied by a phase factor which includes the nucleus-nucleus interaction potential V_{nn} and an additional small correction phase ξ for $z_{\mathrm{final}} = v t_{\mathrm{final}} \to \infty$,

$$A_{IF}(b) = a_{IF}(b)\exp\left[-\frac{i}{v}\left(2\int_0^\infty V_{nn}(R)dz - \xi\right)\right]. \tag{16}$$

The DCS in the center-of-mass (c.m.) system is then given by

$$\left(\frac{d\sigma_{IF}}{d\Omega}\right)_{\mathrm{c.m.}}(\theta) = |f_{IF}^E(\theta)|^2. \tag{17}$$

In the case of the one-electron processes ST and SE a somewhat different model has often been applied. Instead of referring to the IEM it has been assumed that one electron remains in its initial state ϕ_i throughout the collision. If one averages the full two-particle Hamiltonian over the coordinates of the passive electron, one obtains for the Hamiltonian that drives the active electron $\hat{h}_a = \hat{h} + V_{\mathrm{scr}}(R)$ with $\hat{h}$ of Eq. (6) and

$$V_{\mathrm{scr}}(R) = \langle \phi_i | \frac{-Z_p}{r_p} | \phi_i \rangle = -Z_p \int \frac{|\phi_i(r_t)|^2}{|\mathbf{r}_t - \mathbf{R}|} d^3 r_t \tag{18}$$

[23]. This potential does not induce electronic transitions, but accounts for the fact that the projectile scatters from a screened potential [3]. Technically, it modifies the phase factor in Eq. (16) such that

$$A_{IF}^{\mathrm{ST(SE)}}(b) = \sqrt{2} a_{if}^{T(E)}(b)\exp\left[-\frac{i}{v}\left(2\int_0^\infty [V_{nn}(R) + V_{\mathrm{scr}}(R)]dz - \xi\right)\right]. \tag{19}$$

The IEM counterpart of the additional phase is the elastic amplitude a_{ii}^{1s} [cf. Eqs. (13) and (14)]. Obviously, both models coincide if

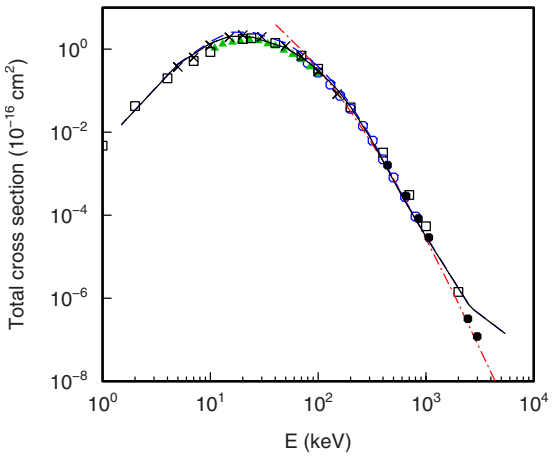

FIG. 1. (Color online) Total single transfer cross section as a function of impact energy for p-He collisions. Theory: solid curve, present TC-BGM calculations within IEM; dashed curve, present TC-BGM calculations within one-active-electron model; dashed-dotted curve: BDW-4B calculation from Mančev *et al.* [2]. Experiments: (□), Barnett [24]; (▲), Shah *et al.* [25]; (○), Shah and Gilbody [26]; (●), Welsh *et al.* [27]; (×), Rudd *et al.* [28].

$$a_{ii}^{1s} = \exp\left[-\frac{i}{v}\left(2\int_0^\infty V_{\mathrm{scr}}(R)dz\right)\right], \tag{20}$$

which corresponds to a dynamic uncoupling of the $1s$ state from all inelastic single-particle channels, i.e., to the uncoupled differential channel equation

$$i\dot{a}_{ii}^{1s} \approx \langle\phi_i|\frac{-Z_p}{r_p}|\phi_i\rangle a_{ii}^{1s}. \tag{21}$$

For comparison we have also used the one-active-electron model (19) for ST and SE calculations with the screening potential of Martin *et al.* [6].

III. RESULTS AND DISCUSSION

A. Single transfer

We begin to present our results with a look at the TCS for ST. In Fig. 1 we compare our results obtained from the IEM and the one-active-electron model with a BDW-four-body (4B) calculation by Mančev *et al.* [2] and with representative measurements, which are selected from the comprehensive collection of data in that work. Both of our curves can hardly be distinguished on the logarithmic plot. Only around the maximum does the IEM yield somewhat smaller cross sections. Compared to the BDW-4B theory the TC-BGM is superior in the low-energy range, which is no surprise given that it is a nonperturbative method. On the other hand, the BDW-4B fares slightly better at energies above approximately 1 MeV. The agreement with experimental data is excellent up to E_P=2 MeV. At higher energies our theory fails, since due to the oscillatory behavior of the electron translation factors very high precision would be necessary to obtain convergent interaction matrix elements. This is a known limitation of all two-center coupled-channel methods for transfer processes [29]. In the following, we restrict ourselves to the energy region 5–200 keV.

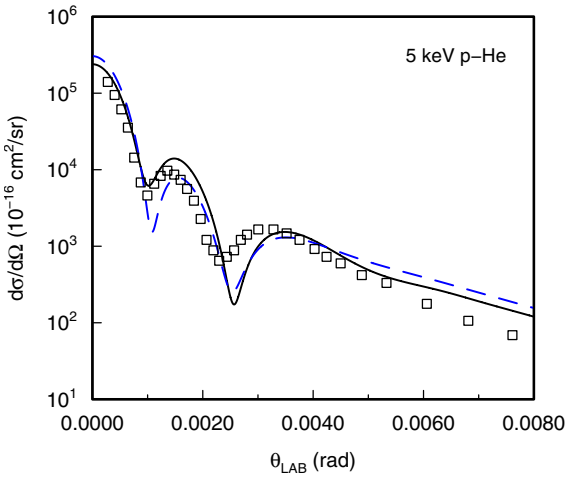

FIG. 2. (Color online) Differential single transfer cross section as a function of laboratory scattering angle for 5 keV p-He collisions. Theory: solid curve, present TC-BGM calculation within IEM; dashed curve, present TC-BGM calculation within one-active-electron model. Experiment: (□), Johnson *et al.* [4].

We start the discussion of DCS at the low-energy end and show results for ST at E_P=5 keV in Fig. 2. Both one- [cf. Eq. (19)] and two-electron models [cf. Eqs. (13) and (16)] give very similar results and describe quite well the characteristic oscillatory structure of Fraunhofer-type diffraction in the experimental data of Johnson *et al.* [4]. In the semiclassical picture the reason for such structures is an interference of the scattering amplitudes caused by transitions between two quasimolecular states in two spatially separated coupling regions in the incoming and outgoing paths of the collision. Although the interference can qualitatively be explained within a two-state approximation, for heavier collision systems it was demonstrated that the presence of other states can significantly affect the phase factor in the transition amplitude [30]. As a result, the positions of the interference extrema sensitively depend on the expansion of the electronic wave function, which may explain the slight differences between theory and experiment. We have also calculated the DCS at E_P=1.5 keV (not shown) and have obtained good agreement with the MO calculations reported by Johnson *et al.* [4]. This can be seen as a confirmation of the ability of our basis to describe the transition processes in slow quasimolecular collisions.

In Figs. 3 and 4 we show calculated DCS for ST at E_P =25–200 keV. In all cases we find structures of varying degrees of significance in the angular region of the Thomas processes, even though the range of impact energies considered rules out significant contributions from these mechanisms. We will comment on the origin of the structures further below, but mention here that similar results have also been obtained when other methods have been employed [1–3]. In our case, it is remarkable that at relatively low impact energies (Fig. 3) the dips are much more pronounced in the IEM than in the one-active-electron model. The comparison with experiment clearly favors the latter, which

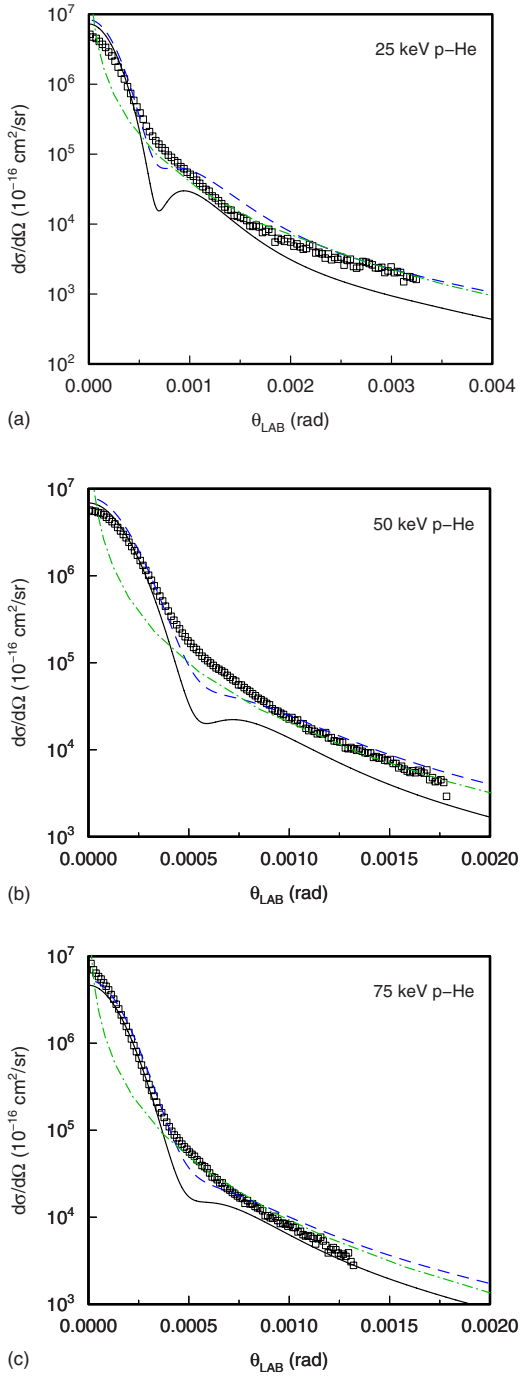

FIG. 3. (Color online) Differential single transfer cross sections as functions of laboratory scattering angle for 25, 50, and 75 keV p-He collisions. Theory: solid curves, present TC-BGM calculations within IEM; dashed curves, present TC-BGM calculations within one-active-electron model; dashed-dotted curves, TC-BGM calculations based on Eq. (2) [9]. Experiments: (□) [31].

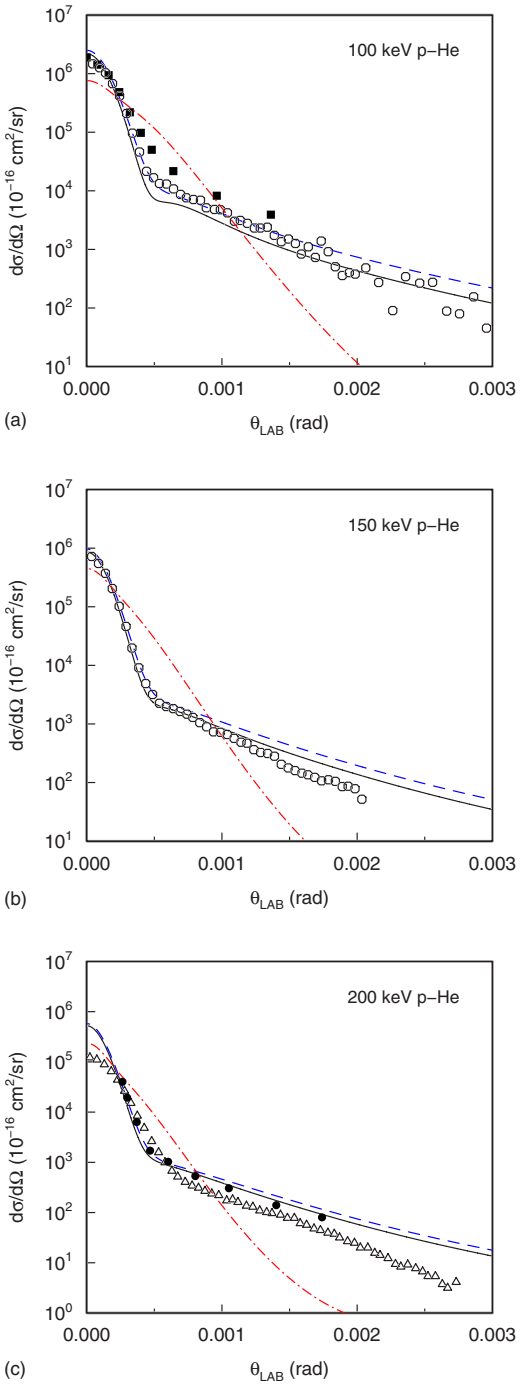

FIG. 4. (Color online) Differential single transfer cross sections as functions of laboratory scattering angle for 100, 150, and 200 keV p-He collisions. Theory: solid curves, present TC-BGM calculations within IEM; dashed curves, present TC-BGM calculations within one-active-electron model; dashed-dotted curves, present TC-BGM calculations within IEM, but without internuclear phase factor. Experiments: (■), Martin *et al.* [6]; (○), Schöffler [33]; (△), Mergel *et al.* [34]; (●), Loftager *et al.* (taken from Mančev *et al.* [2]).

might be taken as an indication that the assumption of independent electrons is not adequate for kinematic situations, in which it is most likely that both electrons end up on different ions. The situation is somewhat reminiscent of the well-known left-right correlation in the dissociation of diatomic molecules, which cannot be described within the IEM [32]. It is also noteworthy that results of a correlated two-electron calculation by Slim *et al.* [5] at $E_P=30$ keV are very similar to the present one-active-electron model data at $E_P=25$ keV.

Furthermore, we have included results obtained from the classical ansatz (2) in Fig. 3. As we have used similar screening potentials in the classical elastic scattering and the quantum mechanical one-active-electron calculations the results merge at large scattering angles as expected from theoretical considerations [12]. Toward smaller scattering angles the classical curves increase monotonically and do not show any structure around $\theta=0.5$ mrad. According to Greenland [12] this approach is limited in our case to $\theta \gg 1/k_i \approx 0.3$ to 0.5 mrad. The data in Fig. 3 qualitatively confirm this criterion, but also suggest that it is not quite as strict since the semiclassical calculation approaches the fully quantum mechanical calculation for $\theta < 1$ mrad.

For $E_P \geq 100$ keV (Fig. 4) the eikonal IEM and one-active-electron model results are rather similar and in good agreement with recent measurements. Following the experimental work [33] we have considered only capture to H($1s$) for our calculations at 100 and 150 keV, whereas all other DCS in Figs. 3 and 4 are inclusive in the final state of the captured electron. We also note that our results at $E_P = 200$ keV compare well with previous calculations of [3], which are not included in the figure for the sake of clarity.

The structures around $\theta=0.5$ mrad are still present at higher energies. From a technical point of view their occurrence is caused by the oscillatory behavior of the Bessel function in the eikonal integral (15), and its interplay with the phases of the electronic amplitude and the nucleus-nucleus (n-n) interaction. The importance of each phase component is different in different angular regions and changes appreciably with impact energy. Only for relatively fast collisions does the situation become sufficiently transparent to allow a straightforward interpretation: for small θ projectile-electron (P-e) interactions dominate, and for large θ, which correspond to close collisions, the n-n interaction is decisive. At intermediate angles around $\theta=0.5$ mrad the interference between both processes becomes most pronounced [21]. To illustrate this interpretation we have calculated the DCS without the n-n phase factor, and indeed the dips disappear for energies $E_P \geq 100$ keV, where any quasimolecular collision picture fails completely.

The above analysis suggests that the theoretical description of features involving the n-n interaction is not completely satisfactory yet. Clearly, it cannot be neglected in the calculations, but on the contrary its adequate inclusion may well be one of the largest remaining problems in atomic collision theory. A similar trend also emerges from recent studies of ionization processes, where unexpected discrepancies between experiment and theory were blamed on an incomplete description of effects involving the n-n interaction [35,36].

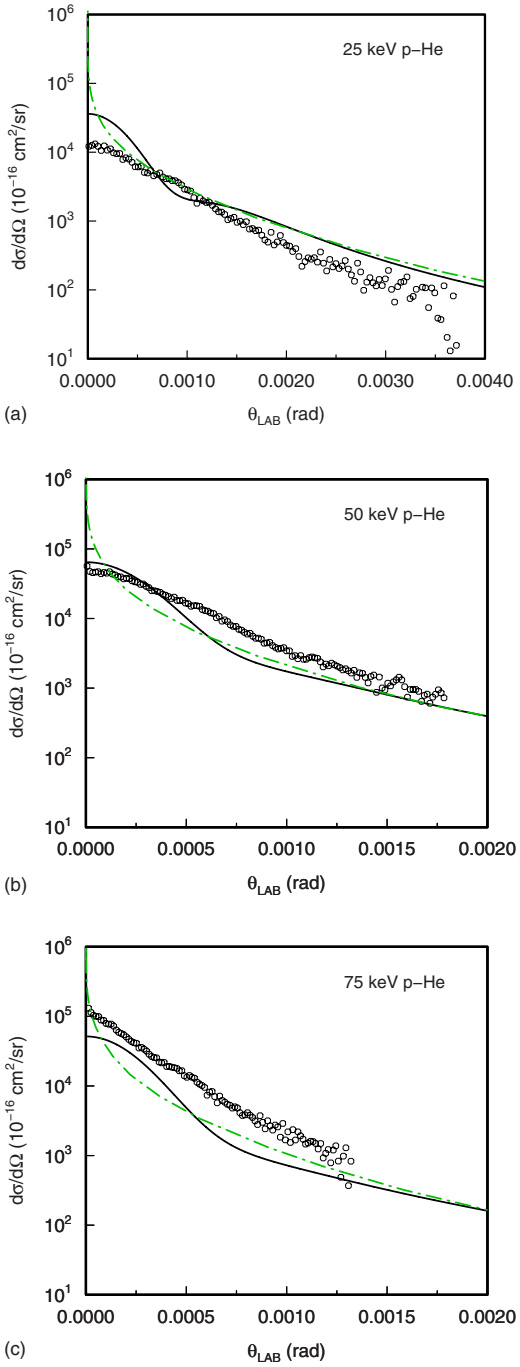

FIG. 5. (Color online) Differential transfer-excitation cross sections as functions of laboratory scattering angle for 25, 50, and 75 keV p-He collisions. Theory: solid curves, present TC-BGM calculations within IEM; dashed-dotted curves, TC-BGM calculations based on Eq. (2) [9]. Experiments: (○) [9].

B. Processes involving target excitation

While ST has been studied quite extensively over many years, DCS for the two-electron TE process have been reported only very recently [9,33]. One can imagine that a variety of correlated mechanisms, such as P-e-e Thomas or shake processes might contribute to TE, but similarly to transfer ionization their domain should be at high impact energies. Therefore, an IEM treatment of TE appears not unreasonable for 25–75 keV proton impact. We have taken this viewpoint in our recent combined experimental and theoretical work [9], and have used the classical ansatz (2) to evaluate the DCS.

In Fig. 5 we show our present eikonal results together with these previous calculations and the measurements. In the calculations we have accounted for capture to the hydro-

gen ground state, and have summed over all final target states up to the N shell, since a differentiation of individual excited states was not possible experimentally. According to our calculation the dominant contribution to TE is due to

$$H^+ + He(1s^2) \rightarrow H^0(1s) + He^+(n=2),$$

which corresponds to the smallest possible energy difference of initial and final states. As in the case of ST the classical and quantum mechanical results are similar at large scattering angles, but the curves have different slopes in the small θ region. The quantum mechanical calculations resemble the behavior of the experimental data somewhat better, but the agreement is less convincing than in the case of ST (cf. Fig. 3). This might signal a shortcoming of the IEM, but it is not clear at present whether one can attribute the deviations to a specific correlated process.

In order to analyze the situation in further detail we compare the ratio of TE to ST cross sections with the corresponding ratio for DE to SE [cf. Eq. (1)]. As mentioned in Sec. I the experimental double ratio R at E_P=50 keV exhibits a peak structure around θ=0.5 mrad, while our previous calculations based on classical heavy-particle scattering yielded monotonically increasing results when different classical screening functions were used for the different processes, and the constant value R=2 for a common scattering potential.

In Fig. 6 we show these previous data together with our present results based on the eikonal approximation. As explained in Sec. II and discussed in Sec. III A for the case of ST we have two possibilities to calculate the one-electron processes: either in the framework of the IEM or in the framework of the one-active-electron models. We have considered both cases (simultaneously) for ST and SE, and do indeed obtain peak structures in R in the θ=0.5 mrad region for both models and all three impact energies considered. The absolute magnitudes of the peaks decrease from E_P =25–75 keV and are larger when all DCS are calculated in the IEM. This is mainly caused by the prominent dips in the IEM results for ST (cf. Fig. 3). Both models are in fair agreement with the experimental data at E_P=50 keV, but it is not possible to decide which one is superior.

In fact, we have found that the peak heights are also quite sensitive to the number of final states included in the calculations for target excitation. Experimentally, only L-shell states are considered for both SE and DE, since in the latter case no significant contributions of higher excited states have been observed. We have restricted the SE calculations accordingly, but in the case of DE we have extended the summations to all $(nln'l')$ combinations up to n=4, since the additional contributions were not negligible. The differential excitation cross sections are shown in Fig. 7. It is interesting that the IEM and one-active-electron model results for SE are in considerably closer agreement with each other than in the case of ST (cf. Fig. 3). In the case of DE the overall agreement with experimental data is better when excited states beyond n=2 are included. As a justification of this procedure we mention that doubly excited IEM states are quite different from correlated ones, such that one should not hope to obtain accurate results for state-to-state transitions in

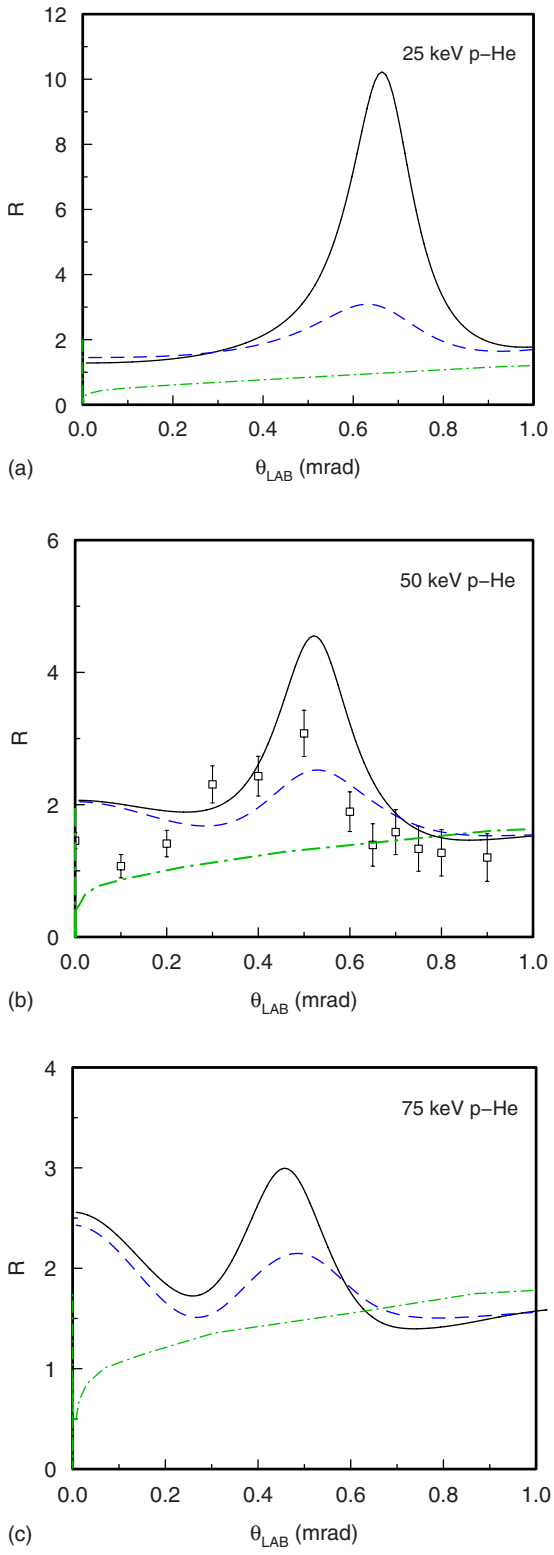

FIG. 6. (Color online) Ratios of transfer-excitation to single transfer versus double to single excitation cross sections [Eq. (1)] as functions of laboratory scattering angle for 25, 50, and 75 keV p-He collisions. Theory: solid curves, present TC-BGM calculations within IEM for all amplitudes; dashed curves, present TC-BGM calculations within one-active-electron models for single transfer and single excitation amplitudes; dashed-dotted curves, TC-BGM calculations based on Eq. (2) [9]. Experiments: (□) [9].

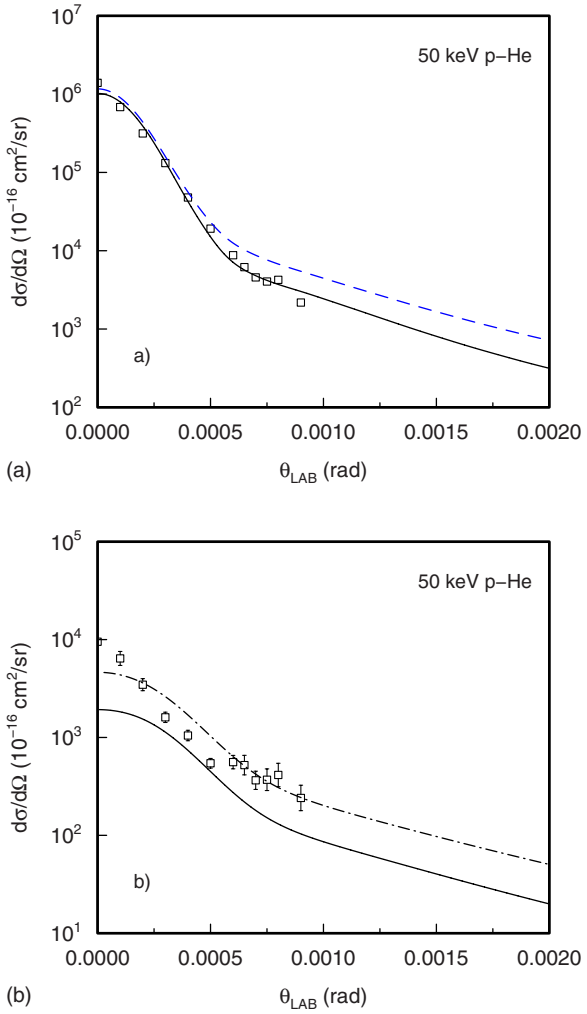

FIG. 7. (Color online) Differential single (a) and double (b) excitation cross sections as functions of laboratory scattering angle for 50 keV p-He collisions. Theory: solid curves, present TC-BGM calculations within IEM; dashed curve, present TC-BGM calculations within one-active-electron model; dashed-dotted curve, present TC-BGM calculations within IEM taking into account all doubly excited states up to $n,n'=4$ (see text). Experiments: (□) [11]. In the case of SE the error bars are smaller than the size of the symbols.

that model, but might obtain a reasonable inclusive DE cross section by summing up all contributions.

Admittedly, this procedure can be criticized, and also in view of the IEM problem with ST and the marginal agreement between calculations and measurements for the case of TE we cannot claim that we have obtained a satisfactory explanation of the experimental peak height of R. It is likely that a better account of the electron-electron interaction in all processes contributing to R is necessary to obtain quantitative agreement with the data. The appearance of the peak, however, is not, or at least not solely, a consequence of such electronic correlations, but is caused by the quantum mechanical heavy-particle-electron couplings, which are taken into account in the eikonal approximation. We reiterate that the structure is completely absent, if the projectile scattering is calculated classically. Furthermore, we note that this conclusion is in line with previous theoretical studies for the ratio of transfer ionization to ST at somewhat higher impact energies [1,21]. Also in that case it was found that IEM calculations produced such structures since the eikonal approximation allows for phase-interference effects between electronic transition amplitudes and the phase of the internuclear interaction potential.

IV. CONCLUSIONS

We have calculated angular-differential cross sections for one- and two-electron processes in p-He collisions within the independent-electron and one-active-electron models. The two-center basis generator method has been used for nonperturbative orbital propagation, and impact-parameter-dependent transition amplitudes have been translated to angular-differential cross sections in the framework of the eikonal approximation. In the case of single transfer we have found overall good agreement with available experimental data over a broad range of impact energies when using the one-active-electron model. Interestingly, the independent electron model seems to overemphasize structures around $\theta=0.5$ mrad below $E_P=100$ keV.

There are still many gaps in our theoretical understanding of two-electron processes, and only reasonable agreement has been obtained for the transfer excitation process and for the double ratio of transfer excitation to single transfer versus double excitation to single excitation. In order to resolve these discrepancies one should probably overcome the independent electron model. However, the appearance of a peak structure in the double ratio at 0.5 mrad does not seem to be connected with electron-electron correlations. Rather, our analysis suggests that this structure is caused by quantum mechanical heavy-particle-electron couplings.

ACKNOWLEDGMENTS

This work was supported in part by the National Science Foundation under Grant No. PHY-0652519. One of the authors (M.Z.) is grateful for financial support from the International Office of the TU Clausthal financed by the German Academic Exchange Service.

[1] D. Belkić, *Principles of Quantum Scattering Theory* (Institute of Physics, Bristol, 2003).
[2] I. Mančev, V. Mergel, and L. Schmidt, J. Phys. B **36**, 2733 (2003).
[3] P. Abufager, P. D. Fainstein, A. E. Martínez, and R. D. Rivarola, J. Phys. B **38**, 11 (2005).
[4] L. K. Johnson, R. S. Gao, R. G. Dixson, K. A. Smith, N. F. Lane, R. F. Stebbings, and M. Kimura, Phys. Rev. A **40**, 3626 (1989).
[5] H. A. Slim, E. L. Heck, B. H. Bransden, and D. R. Flower, J. Phys. B **24**, 2353 (1991).
[6] P. J. Martin, K. Arnett, D. M. Blankenship, T. J. Kvale, J. L. Peacher, E. Redd, V. C. Sutcliffe, J. T. Park, C. D. Lin, and J. H. McGuire, Phys. Rev. A **23**, 2858 (1981).
[7] J. Ullrich, R. Moshammer, A. Dorn, R. Dörner, L. P. H. Schmidt, and H. Schmidt-Böcking, Rep. Prog. Phys. **66**, 1463 (2003).
[8] H. Schmidt-Böcking *et al.*, Nucl. Instrum. Methods Phys. Res. B **233**, 3 (2005).
[9] A. Hasan, B. Tooke, M. Zapukhlyak, T. Kirchner, and M. Schulz, Phys. Rev. A **74**, 032703 (2006).
[10] W. T. Htwe, T. Vajnai, M. Barnhart, A. D. Gaus, and M. Schulz, Phys. Rev. Lett. **73**, 1348 (1994).
[11] M. Schulz, W. T. Htwe, A. D. Gaus, J. L. Peacher, and T. Vajnai, Phys. Rev. A **51**, 2140 (1995).
[12] P. T. Greenland, J. Phys. B **14**, 3707 (1981).
[13] M. Zapukhlyak, T. Kirchner, H. J. Lüdde, S. Knoop, R. Morgenstern, and R. Hoekstra, J. Phys. B **38**, 2353 (2005).
[14] R. McCarroll and A. Salin, J. Phys. B **1**, 163 (1968).
[15] L. Wilets and S. J. Wallace, Phys. Rev. **169**, 84 (1968).
[16] R. J. Glauber, *Lectures in Theoretical Physics* (Interscience, New York, 1959), Vol. 1, pp. 315–414.
[17] E. Engel and S. H. Vosko, Phys. Rev. A **47**, 2800 (1993).
[18] H. J. Lüdde, A. Henne, T. Kirchner, and R. M. Dreizler, J. Phys. B **29**, 4423 (1996).
[19] O. J. Kroneisen, H. J. Lüdde, T. Kirchner, and R. M. Dreizler, J. Phys. A **32**, 2141 (1999).
[20] T. Kirchner, H. J. Lüdde, and M. Horbatsch, Recent Res. Dev. Phys. **5**, 433 (2004).
[21] R. Gayet and A. Salin, Nucl. Instrum. Methods Phys. Res. B **56-57**, 82 (1991).
[22] B. H. Bransden and M. R. C. McDowell, *Charge Exchange and the Theory of Ion-Atom Collisions* (Clarendon, Oxford, 1992).
[23] P. D. Fainstein, V. H. Ponce, and R. D. Rivarola, J. Phys. B **21**, 287 (1988).
[24] *Redbook. Atomic Data for Fusion*, edited by C. F. Barnett (ORNL, New York, 1990), Vol. 1, http://www-cfadc.phy.ornl.gov/redbooks/redbooks.html
[25] M. B. Shah, P. McCallion, and H. B. Gilbody, J. Phys. B **22**, 3037 (1989).
[26] M. B. Shah and H. B. Gilbody, J. Phys. B **18**, 899 (1985).
[27] L. M. Welsh, K. H. Berkner, S. N. Kaplan, and R. V. Pyle, Phys. Rev. **158**, 85 (1967).
[28] M. E. Rudd, R. D. DuBois, L. H. Toburen, C. A. Ratcliffe, and T. V. Goffe, Phys. Rev. A **28**, 3244 (1983).
[29] J. Eichler, *Lectures on Ion-Atom Collisions* (Elsevier, Amsterdam, 2005).
[30] R. Schuch, H. Ingwersen, E. Justiniano, H. Schmidt-Böcking, M. Schulz, and F. Ziegler, J. Phys. B **17**, 2319 (1984).
[31] M. Schulz, T. Vajnai, and J. A. Brand, Phys. Rev. A **75**, 022717 (2007).
[32] F. L. Pilar, *Elementary Quantum Chemistry* (McGraw-Hill, New York, 1968).
[33] M. Schöffler, Ph.D. thesis, Johann Wolfgang Goethe-Universität, 2006 (unpublished).
[34] V. Mergel, R. Dörner, K. Khayyat, M. Achler, T. Weber, O. Jagutzki, H. J. Lüdde, C. L. Cocke, and H. Schmidt-Böcking, Phys. Rev. Lett. **86**, 2257 (2001).
[35] M. Schulz, R. Moshammer, D. Fischer, H. Kollmus, D. H. Madison, S. Jones, and J. Ullrich, Nature (London) **422**, 48 (2003).
[36] N. V. Maydanyuk, A. Hasan, M. Foster, B. Tooke, E. Nanni, D. H. Madison, and M. Schulz, Phys. Rev. Lett. **94**, 243201 (2005).